

Unique Properties of Selectively Formed Zirconia Nanostructures

By James L. Gole,* Sharka M. Prokes, John D. Stout, Orest J. Glembocki, and Rusen Yang

Zirconia has attracted considerable attention because of its diverse practical applications in fuel-cell technology,^[1] its use as a catalyst or catalyst support,^[2] its ability to combine with sulfuric acid to form extremely strong acids,^[3] and its use as an oxygen sensor^[4] and as a possible high-dielectric-constant material for large-scale integrated circuits or as a gate dielectric in metal-oxide semiconductor devices.^[5,6] However, the optical properties^[7,8] of this semiconductor, especially its photoluminescence (PL) properties, are seldom reported. Because these PL properties, if properly harnessed, might play an important role in the future improvement of information-storage devices,^[9–13] the characterization and enhancement of PL from ZrO_x may have important implications. Here, we expand the potential of these optical properties.

We report not only on the formation of nanometer-sized ZrO_x structures which combine into fractal forms, but also on the first synthesis procedure for preparing zirconia-based nanoshells and hollow nanospheres. Our synthesis procedure complements recent spray-pyrolysis studies, which produce hollow nanospheres in the size range 1–10 μm .^[14] The formation and growth of nanoshells and nanospheres can greatly dominate the formation of other less-defined zirconia-based nanostructures under certain experimental conditions. The nanoshells produced do not result from solvent-induced nanosphere disruption^[14] and they have smooth, as opposed to fractured, surfaces. In contrast to zirconia-based nanoparticles and nanospheres, we find that these “metal-oxide” nanoshell configurations demonstrate a significantly enhanced PL that may result from the geometry of the ultrathin nanoshell walls.

In Figures 1a–c, we present representative transmission electron microscopy (TEM) images corresponding to the irregularly shaped and distorted spheroidal structures typically formed under a wide range of experimental conditions. These spheroidal structures readily combine into the fractal-like structure depicted in Figure 1c. In contrast, Figures 2a–e present representative TEM images corresponding to the ZrO_x nanoshell and nanospherical forms, which we generated under a set of specific conditions outlined in the Experimental section. These structures should be compared to the nanostructures

depicted in Figure 1, which are formed over a much wider range of conditions. Figure 2a represents an overview of nanoshell and nanosphere formation accompanied by the formation of a few hollow elliptical forms. Figure 2b presents a closer view obtained from a spectrum taken of material formed under similar conditions demonstrating both thick- (~20 nm) and thin- (~5 nm) walled shell formation. We found that thick-walled shells can be generated and grown in regions of slower condensation between a source reactant oxidant nozzle- ($ZrCl_4$) containing crucible and a downstream cold finger at ~20 °C. More rapid condensation at the cold finger, enhanced by a larger temperature gradient relative to the reactant oxidation zone, produces thinner-walled shells and some hollow spheres. Figure 2c represents the arrested formation of a hollow nanosphere as it grows from a thick-walled nanoshell in the region (downstream) intermediate to the reaction/oxidation zone and the system cold finger. By examining product formation across this region under appropriate conditions, it is possible to observe several degrees of growth. Provided that initially forming shells diffuse to the cold finger they can be surrounded by a thin-walled shell (Fig. 2d). Figure 2d exemplifies several multishelled/-walled configurations oriented about a central nanosphere where the outer nanoshell is thin-walled. Figure 2e demonstrates a smaller nanosphere located within a thick-walled, nearly nanospherical shell-like structure. A closer view of the hollow nanosphere groupings reveals that they can be interconnected by a permeable channel.

In Figures 3a–c Raman spectra taken for the ZrO_x nanoshell- and hollow-nanosphere configurations can be compared. Figure 3a corresponds to the Raman spectrum and curve fit for ZrO_x nanoshells (see Fig. 2b). The curve-fit spectrum is dominated by features associated with crystalline tetragonal (475 620 cm^{-1}) and monoclinic^[15–17] ZrO_x . The features associated with the spectrum of crystalline tetragonal nanoshells are shifted from those of ZrO_x powder (Fig. 3c), where they are located at 477.5 and 616.45 cm^{-1} . The Raman spectrum observed for samples generated under conditions that favor the formation of nanospheres (Fig. 3b) appears to correspond to a broad peak located near 570 cm^{-1} . This result suggests that the crystallinity associated with the nanoshells is lost in sphere formation (Figs. 2c–e), as these structures are amorphous in character. We have not yet obtained evidence that a crystalline structure can be associated with either the irregular nanostructures of Figure 1 or the formed nanospheres. For comparison, Figure 3c shows the corresponding Raman spectrum of bulk ZrO_x powder. The observed features are in agreement with the observations of previous workers.^[15] Not

[*] Dr. J. L. Gole, J. D. Stout, R. Yang
School of Physics, Georgia Institute of Technology
Atlanta, GA 30332-0430 (USA)
E-mail: jim.gole@physics.gatech.edu
Dr. S. M. Prokes, Dr. O. J. Glembocki
Naval Research Laboratory
Washington, DC 20375-5000 (USA)

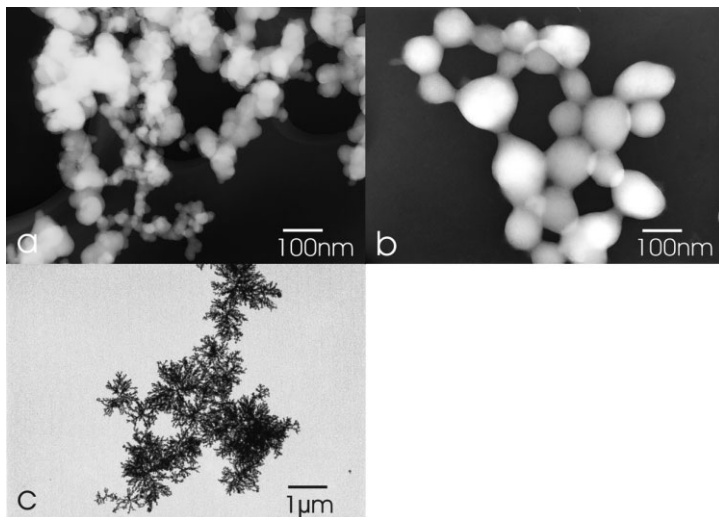


Figure 1. TEM images of ZrO_x nanostructures: a) irregular nanostructures with partial agglomeration, b) spheroidal nanostructures (≤ 5 nm), and c) fractal structure of nanostructure agglomeration.

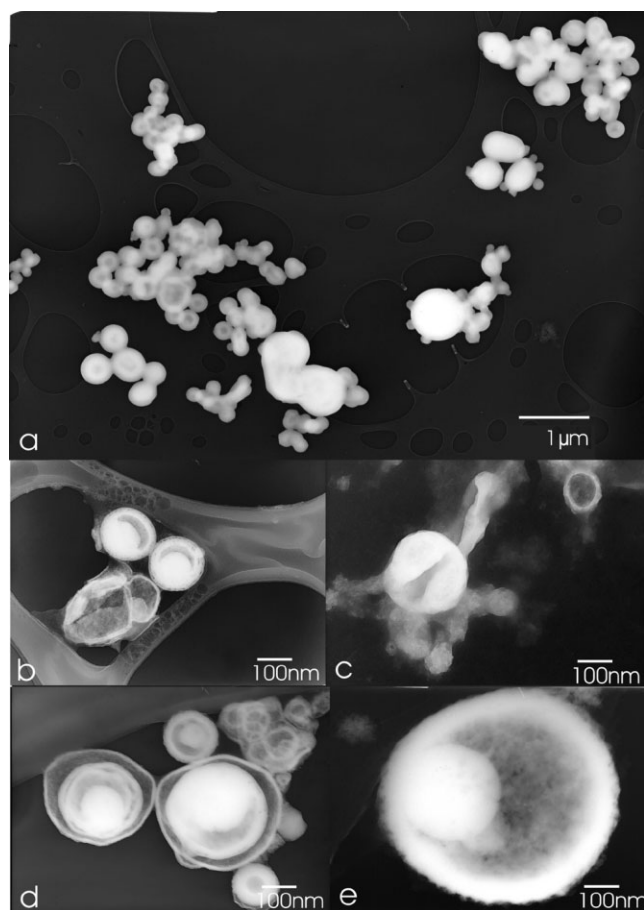


Figure 2. TEM images of ZrO_x nanostructures: a) overview of nanoshells and hollow nanospheres, and their distribution; b) closer view of variable-wall-thickness nanoshells; c) arrested formation of a nanosphere; d) interlocked nanoshell/nanosphere configurations; and e) thick-walled hollow nanospheres within forming nanospheres.

surprisingly, the Raman features associated with the ZrO_x nanoshells are considerably broader than those associated with ZrO_2 powders.

The differences between the ZrO_x nanoshells, nanospheres, and irregularly shaped nanostructures are starkly evident in PL intensity measurements. Figure 4 presents the PL from ZrO_x nanoshells and the corresponding emission from nanospheres and irregularly shaped nanostructures. Because the direct-band PL in ZrO_2 occurs at 390 nm for the tetragonal and 475 nm for the monoclinic phases,^[18] the feature near 575 nm in Figure 4 is most likely due to an oxygen defect site.^[19] Note that it is 56.41 times more intense for comparable samples of the nanoshell material than for the nanospheres (Figs. 2a,c), and for the irregularly shaped nanostructures depicted in Figure 1. Furthermore, if one takes into account the volume differences between the nanoshells and nanospheres, there is an additional factor of 12.7 times more material per unit volume for the nanospheres. If we normalize the PL in Figure 4 to the volume, we find that the PL for the nanoshell geometry is 716 times more intense than that of the nanospheres. The observed PL is also significantly more intense than the PL associated with crystalline ZrO_2 powders (Raman spectrum shown in Fig. 3c).

One possible explanation for this result is the reduction of non-radiative recombination centers. This is consistent with the crystalline quality of the nanoshells compared to that of the nanospheres, as shown by the Raman spectra in Figure 3. Since the Raman spectra of the nanoshells exhibit well-defined lines, while the nanosphere Raman spectrum shows only one broad and weak feature, we speculate that the crystalline quality of the nanoshell is significantly better. Thus, we would expect a significant reduction in non-radiative recombination centers due to an improved crystallinity. This could account for some of the PL enhancement.

One possible explanation for this result is the reduction of non-radiative recombination centers. This is consistent with the crystalline quality of the nanoshells compared to that of the nanospheres, as shown by the Raman spectra in Figure 3. Since the Raman spectra of the nanoshells exhibit well-defined lines, while the nanosphere Raman spectrum shows only one broad and weak feature, we speculate that the crystalline quality of the nanoshell is significantly better. Thus, we would expect a significant reduction in non-radiative recombination centers due to an improved crystallinity. This could account for some of the PL enhancement.

An alternate explanation is that the non-bridging oxygen hole center (NBOHC) defect is confined to the surface, as demonstrated in other nanoscale systems.^[20] For such a case, the photoexcited electrons must diffuse to the surface in order to recombine. This process depends greatly on the diffusion length of the carriers, and must be compared to the distance of these carriers from the surface. By reducing the distance to the surface, as in the case of the nanoshell geometry, one can significantly increase the probability of recombination at the surface NBOHCs. Furthermore, the crystal quality will determine the electron diffusion length. From the discussion above, we would expect a significant reduction in non-radiative recombination centers for the shell geometry, as the thin shell thickness should greatly enhance the probability of recombination. Furthermore, this model would account for the differences in PL between the powders and the nanoshells, because the powders also consist of material of high crystallinity, yet their PL is a factor of 30 times lower. However, at this point, we cannot distinguish between the two mechanisms, and it is possible that both mechanisms play a role in the significant PL enhancement we observe.

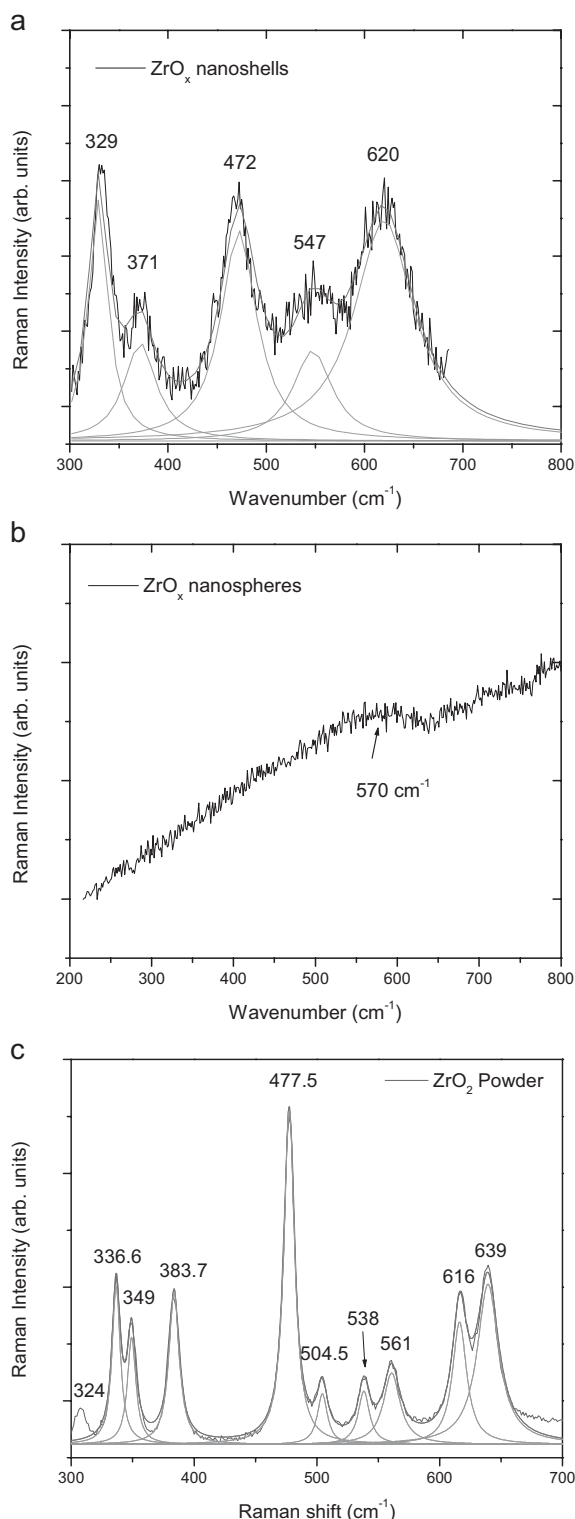


Figure 3. Raman spectra of a) ZrO_x nanoshells (shown in Fig. 1b), b) ZrO_x nanospherical shapes (Figs. 2a,c), and c) ZrO₂ powder.

We have successfully generated ZrO_x nanoshells that display a greatly enhanced defect site PL and we have shown that the nanoshell geometry results in better crystalline and electronic material quality. The ability to generate hollow

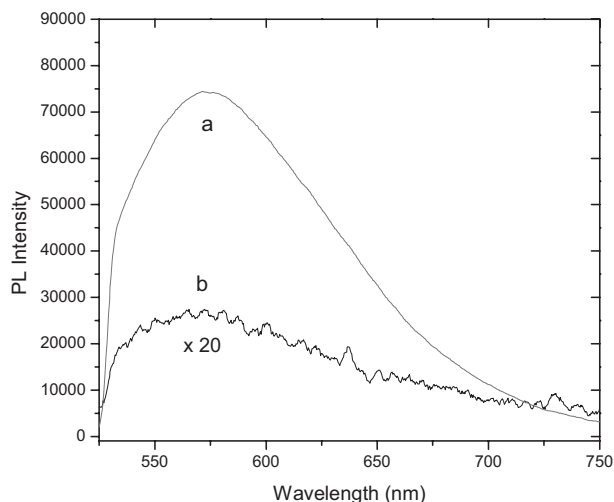


Figure 4. PL emission excited by the 514.5 nm line of an argon-ion laser (25 mW) for ZrO_x nanoshells (a) and ZrO_x nanospheres (b). The PL from the nanoshells is 56.4 times more intense.

nanospheres (see Lenggoro et al.) may provide a medium for fuel-cell applications,^[1] hydrogen storage,^[21] and thermo-power applications.^[22] The ZrO_x nanospheres also appear to have porous walls. If hydrogen can diffuse into these hollow structures, which represent sufficiently porous metal oxides, and this process can convert the inner-wall metal-oxide surface to an oxyhydride, decreasing the wall porosity significantly so as to considerably abate diffusion of hydrogen from the central region of the hollow spheres, a storage medium might be created. Further heating might then be used to convert the oxyhydride to the oxide with subsequent release of hydrogen. Finally, we note that the nature of arrested nanosphere formation, as exemplified in Figure 2c, offers the possibility for arrested gas diffusion through a partially closed structure; this process might improve the efficiency of ZrO₂-based catalyst and catalyst support configurations.

In addition, Oldenberg,^[23] in his study of light scattering from gold nanoshells, found that by adjusting the ratio of the radius of the dielectric core to the thickness of the shell, he was able to tune the gold plasma resonance from 500 to 2500 nm. This tuning should vary with the dielectric core. Oldenberg, Halas and co-workers^[23,24] used gold sulfide and silica-core dielectrics. We propose that it would be of interest to compare their results with those obtained with a much higher K dielectric, such as that of ZrO₂.

In summary, unique ZrO_x nanoshells and nanospheres have been formed over a precise range of temperature and pressure. The nanoshells exhibit a greatly enhanced PL which is well in excess of 100 times that of either the nanospheres or irregularly shaped ZrO₂ nanoparticles. This enhanced PL may be related to the nanoshell geometry. The nanoshells can be further transformed to a variety of hollow nanospheres, small numbers of which can be made to agglomerate to interconnected chamber arrays. Potential applications of the nanoshells, the hollow ZrO_x nanospheres, and their intermediates have been considered.

Experimental

The preparation of ZrO_x nanoshells and hollow nanospheres requires that we find a “sweet zone” for the synthesis. ZrO_x is prepared from the oxidation of $ZrCl_4$ primarily with O_2 . An argon/oxidant mix was made to flow over a crucible filled with $ZrCl_4$ in the central region of a modified-tube furnace configuration [25,26]. To produce ZrO_x nanoshells and hollow nanospheres, we required operation at a $ZrCl_4$ temperature between 305 and 325 °C (corresponding to sublimation) depending on the particular oxidant nozzle or nozzle array used in the experiment. These temperatures are somewhat below the melting point of 331 °C. The gas flow rate was also varied with nozzle configuration and was optimal when close to 12 standard cubic centimeters per minute (sccm) of argon was combined with between three (smaller nozzle) and 8 sccm (flow array) of oxygen. The optimal helium entrainment gas tube furnace pressure was less than 300 torr (1 torr = 133.32 Pa) but greater than 100 torr. If the system was operated at a “crucible” temperature less than 300 °C, little product was formed. However, if the system was operated at temperatures greater than 330 °C shells and hollow spheres were not readily produced; on the contrary, ZrO_2 particulates of various sizes were formed. The placement of the oxidant nozzle source above the crucible was also significant as the argon entrained oxidant must flow efficiently onto the gaseous $ZrCl_4$ created by the sublimation process. A given oxidant nozzle was placed over the central region of the crucible containing $ZrCl_4$ or in a position further downstream in the direction of the flow and somewhat closer to the system cold finger [25,26] and the preceding region onto which both the shells and hollow spheres condense. If the oxidizing nozzle was placed completely upstream from the crucible or if the array was rotated so that the argon/oxygen (oxidant) mix did not flow directly onto the subliming $ZrCl_4$ mix, considerably smaller semiporous nanostructures appeared to form.

We have combined TEM and Raman and PL spectroscopy to demonstrate the significantly enhanced PL associated with spatial carrier confinement within the ultrathin nanoshell walls. TEM analysis was carried out at 100 KV using a JEOL 1000 TEM. The confocal micro-Raman system that was used consisted of a Mitutoyo microscope and a SPEX Triplemate spectrometer equipped with a charge-coupled device. The 514.5 nm line of an Ar-ion laser was used as the excitation source and the laser had a power of 25 mW or less. The microscope had 10×, 50×, and 100× objectives for focusing the laser light and was coupled to the spectrometer through a fiber-optic bundle. The light from the microscope was filtered by a 514.5 nm notch filter. The positions of the Raman lines in a given spectrum were calibrated against the 546.0 nm line emission from a fluorescent light source. Comparative PL behavior for virtually identical sized samples was evaluated using the 514.5 nm line of the Ar-ion laser and detection of the PL was performed using an Ocean Optics spectrometer with an optical-fiber light collection system. A 514.5 nm notch filter was used to ensure that the laser line did not enter the spectrometer or detector.

Received: April 15, 2005

Final version: December 1, 2005

- [1] A. H. Heuer, L. W. Hobbs, *Science and Technology of Zirconia, Advances in Ceramics*, Vol. 3, American Ceramic Society, Columbus, OH 1981.
- [2] Y. W. Li, D. H. He, Z. X. Cheng, C. L. Su, J. R. Li, M. Zhu, *J. Mol. Catal. A* **2001**, 175, 267.
- [3] M. G. White, unpublished results.
- [4] E. C. Subbarao, H. S. Maiti, *Adv. Ceram.* **1988**, 24, 731.
- [5] T. S. Kalkur, Y. C. Lu, *Thin Solid Films* **1992**, 193, 207.
- [6] G. D. Wilk, R. M. Wallace, *Appl. Phys. Lett.* **2000**, 112, 76.
- [7] A. V. Emeline, A. V. Rudakova, V. K. Ryabchuk, N. Serpone, *J. Phys. Chem. B* **1998**, 102, 10906.
- [8] R. H. French, S. J. Glass, F. S. Ohuchi, Y.-N. Xu, W. Y. Ching, *Phys. Rev. B* **1994**, 49, 5133.
- [9] *Informational Materials*, Tianjin University Press (Ed: F. X. Gan), Tianjin, P. R. China **2000**.
- [10] M. H. Huang, S. Mao, H. Feick, H. Yan, Y. Wu, E. Weber, R. Russo, P. Yang, *Science* **2001**, 292, 1897.
- [11] M. H. Huang, Y. Wu, H. Feick, N. Tran, E. Weber, P. Yang, *Adv. Mater.* **2001**, 13, 113.
- [12] Y. C. Kong, D. P. Yu, B. Zhang, W. Fang, S. Q. Feng, *Appl. Phys. Lett.* **2001**, 78, 407.
- [13] Y. Li, G. M. Meng, L. D. Zhang, F. Phillipp, *Appl. Phys. Lett.* **2000**, 76, 2011.
- [14] I. W. Lenggoro, T. Hata, F. Iskandar, M. M. Lunden, K. Okuyama, *J. Mater. Res.* **2000**, 15, 733.
- [15] C. Carlone, *Phys. Rev. B* **1992**, 45, 2079.
- [16] R. Gomez, T. Lopez, X. Bokhimi, E. Munoz, J. L. Boldu, O. Navaro, *J. Sol-Gel Sci. Technol.* **1998**, 11, 309.
- [17] J. A. Wang, M. A. Valenzuela, J. Salmones, A. Vazquez, A. Garcia-Ruiz, X. Bokhimi, *Catal. Today* **2001**, 68, 21.
- [18] L.-J. Lai, H.-C. Lu, H.-K. Chen, B.-M. Cheng, M.-I. Lin, T.-C. Chu, *J. Electron Spectrosc. Relat. Phenom.* **2005**, 144–147, 865.
- [19] S. M. Prokes, J. L. Gole, C. Burda, X. Chen, W. E. Carlos, *Adv. Funct. Mater.* **2005**, 15, 161.
- [20] S. M. Prokes, W. E. Carlos, O. J. Glembocki, *Phys. Rev. B* **1994**, 50, 17093.
- [21] *Advanced Materials for Energy Conversion II* (Eds: D. Chandra, R. G. Bautista, L. Schlapbach), The Minerals, Metals, and Materials Society, Warrendale, PA **2004**.
- [22] K. T. Wojciechowski, J. Oblakowski, *Solid State Ionics* **2003**, 157, 341.
- [23] J. Oldenborg, *Ph.D. Thesis*, Rice University **2000**.
- [24] J. Jackson, S. Westcott, L. Hirsch, N. Halas, *American Physical Society*, presented at Joint Fall Meetings of the Texas Sections of the APS, and APPT, Zone 13 of the SPS, and the National Society of Hispanic Physicists, Rice University, Houston, Texas Meeting ID: TSF00, abstract #B1.007, October **2000**.
- [25] a) J. L. Gole, J. D. Stout, W. L. Rauch, Z. L. Wang, *Appl. Phys. Lett.* **2000**, 76, 2346. b) R. O. Gao, Z. L. Wang, J. L. Gole, J. D. Stout, *Adv. Mater.* **2000**, 12, 1938.
- [26] J. L. Gole, Z. L. Wang, Z. R. Dai, J. D. Stout, R. P. Gao, M. White, *Prog. Colloid Polym. Sci.* **2003**, 281, 673.